THE JOURNAL OF BIOLOGICAL CHEMISTRY VOL. 283, NO. 44, pp. 30341–30350, October 31, 2008

Ciliary Neurotrophic Factor, Cardiotrophin-like Cytokine, and Neuropoietin Share a Conserved Binding Site on the Ciliary Neurotrophic Factor Receptor α Chain*[S]

Received for publication, April 28, 2008, and in revised form, August 25, 2008 Published, JBC Papers in Press, August 26, 2008, DOI 10.1074/jbc.M803239200

François Rousseau[1], **Sylvie Chevalier, Catherine Guillet, Elisa Ravon, Caroline Diveu, Josy Froger, Fabien Barbier, Linda Grimaud, and Hugues Gascan**[2]

From the Unité Mixte INSERM 564, Bâtiment Monteclair, 4 Rue Larrey, 49033 Angers Cedex 01, France

Ciliary neurotrophic factor, cardiotrophin-like cytokine, and neuropoietin are members of the four-helix bundle cytokine family. These proteins signal through a common tripartite receptor composed of leukemia inhibitory factor receptor, gp130, and ciliary neurotrophic factor receptor α. Binding to ciliary neurotrophic factor receptor α occurs through an interaction site located at the C terminus of the cytokine AB loop and αD helix, known as site 1. In the present study, we have generated a model of neuropoietin and identified a conserved binding site for the three cytokines interacting with ciliary neurotrophic factor receptor α. To identify the counterpart of this site on ciliary neurotrophic factor receptor α, its cytokine binding domain was modeled, and the physicochemical properties of its surface were analyzed. This analysis revealed an area displaying properties complementary to the site 1 of ciliary neurotrophic factor, cardiotrophin-like cytokine, and neuropoietin. Based on our computational predictions, residues were selected for their potential involvement in the ciliary neurotrophic factor receptor α binding epitope, and site-directed mutagenesis was carried out. Biochemical, cell proliferation, and cell signaling analyses showed that Phe^{172} and Glu^{286} of ciliary neurotrophic factor receptor α are key interaction residues. Our results demonstrated that ciliary neurotrophic factor, cardiotrophin-like cytokine, and neuropoietin share a conserved binding site on ciliary neurotrophic factor receptor α.

Ciliary neurotrophic factor (CNTF),[3] cardiotrophin-like cytokine (CLC), and neuropoietin (NP) belong to the interleukin-6 family of cytokines. This family also includes leukemia-inhibitory factor (LIF), oncostatin M, IL-11, IL-27, and cardiotrophin-1 (1–6). CNTF, CLC, and NP form a subfamily of proteins using the same tripartite receptor, and their bioactivities are mainly restricted to the nervous system (7).

In particular, CNTF maintains motor neuron viability *in vitro*, prevents the degeneration of axotomized motor neurons, and attenuates motor deficits in different strains of mice with neuromuscular deficiencies (8–13). It is also a protective factor in demyelinating central nervous system disease (14). In addition to its activities in the nervous system, CNTF has trophic effects on denervated skeletal muscle and is a regulator of muscular strength in aging (15, 16). Other findings show that CNTF is also a potential agent in the treatment of diabetes as well as obesity (17, 18).

CLC, a CNTF paralog, shares 37% similarity with CNTF (19). We previously showed that CLC forms a composite cytokine when it is associated with the soluble receptor cytokine-like factor 1. Cytokine-like factor 1 mainly behaves as a chaperone protein, allowing secretion of CLC (2). Subsequently, we observed that CLC can form a second secreted composite cytokine when associated with the soluble form of CNTFRα (20).

We have recently reported inactivating mutations in the *CLC* gene of a patient suffering from cold-induced sweating syndrome (21). This syndrome is characterized by a profuse sweating after exposure to cold. This patient also displays congenital physical abnormalities, degenerative disease of the cervical and lumbar spine, and a mild sensorimotor peripheral neuropathy.

NP, the third CNTF paralog identified by our group (1), is expressed concomitantly and co-localized with CNTFRα in the mouse embryo, suggesting a key role in nervous system development. However, a deletion of 8 nucleotides inactivates the NP gene (*NP*) in humans. This finding suggests that *NP* has evolved into a pseudogene in humans.

To exert their biological functions, CNTF, CLC, and NP bind to a tripartite receptor complex, which includes gp130- and LIFR-transducing chains associated with the aforementioned specific α-binding chain, CNTFRα (1, 2, 22–25). This specific α chain exists either in a soluble or GPI-anchored membrane form, which in both cases contributes to gp130 and LIFR recruitment by CNTF and to its subsequent biological response (26, 27). The consequent signaling events involve the recruitment and activation of the Janus kinase/signal transducer and activator of transcription (STAT) pathways (3, 28–30).

gp130, LIFR, and CNTFRα are members of the class I hematopoietin receptor family. This family of receptors is defined by a modular structure and characterized by a cytokine binding

* This work was supported by Association Française contre les Myopathies Grant 9884 and by the Ciblage Moléculaire et Application Thérapeutique (CIMATH) program of the region Pays de la Loire. The costs of publication of this article were defrayed in part by the payment of page charges. This article must therefore be hereby marked "*advertisement*" in accordance with 18 U.S.C. Section 1734 solely to indicate this fact.

[S] The on-line version of this article (available at http://www.jbc.org) contains supplemental Fig. 1.

[1] Supported by the Angers Agglomeration.

[2] To whom correspondence should be addressed. Tel.: 33-2-41-35-47-31; Fax: 33-2-41-73-16-30; E-mail: hugues.gascan@univ-angers.fr.

[3] The abbreviations used are: CNTF, ciliary neurotrophic factor; CLC, cardiotrophin-like cytokine; NP, neuropoietin; LIF, leukemia-inhibitory factor; IL, interleukin; STAT, signal transducer and activator of transcription; CBD, cytokine binding domain; mAb, monoclonal antibody; WT, wild type.

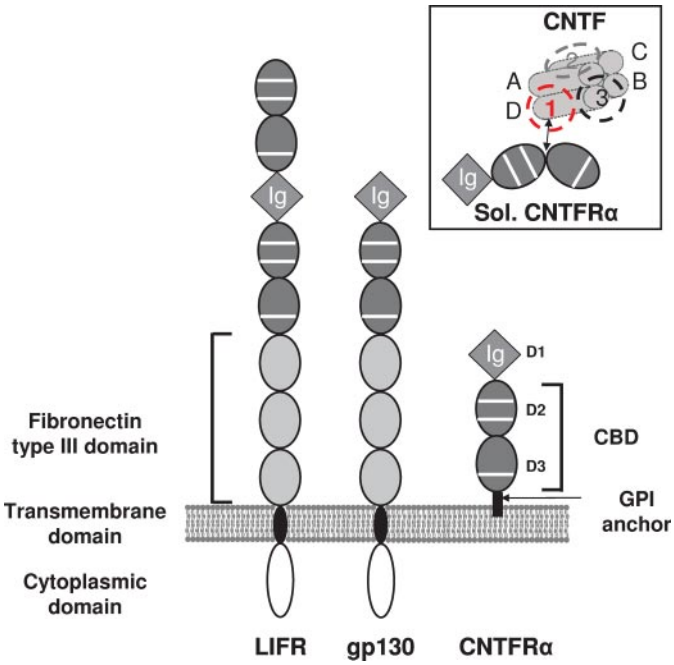

FIGURE 1. **Schematized view of the domain structure of CNTF, LIFR, gp130, and CNTFRα and representation of CNTF/CNTFRα interaction.** The Ig-like domain, CBD, and fibronectin type III domain are represented as a *gray square*, *dark gray circle*, and *light gray circle*, respectively. The positions of CNTF binding sites are indicated. *GPI*, glycosylphosphatidylinositol.

domain (CBD) (31, 32). The CBD is composed of two "specialized" fibronectin III domains linked by a proline-rich sequence (Fig. 1). The N-terminal fibronectin III domain of the CBD (the D2 domain in Fig. 1) is characterized by two conserved disulfide bridges. The C-terminal fibronectin III domain of the CBD (the D3 domain in figure 1) contains a conserved WS*X*WS motif. The crystal structure of several type I cytokine receptors and cytokine-receptor complexes has revealed that CBD forms an elbow-shaped module bent at an angle of ~90°. The receptor CBD interacts with cytokines through loops located at the boundary of the two fibronectin III domains (33).

The IL-6 family of cytokines belongs to the "long chain" four-α helix bundle class, with an up-up down-down topology (7). The different secondary structures are named A–D from the N terminus to C terminus (Fig. 1). Crystallographic structures and site-directed mutagenesis studies have shown that these cytokines interact with their receptor through three different binding sites, numbered 1–3 by analogy with growth hormone (Fig. 1) (34, 35). Cytokines requiring an α chain, like CNTF, CLC, NP, IL-6, and IL-11, bind first to the receptor through a site 1 composed of residues from the C-terminal parts of the AB loop and the αD helix (Fig. 1).

Site 2 is located on solvent-exposed faces of the αA and αC helices and is important for binding to gp130. Site 3 is specific to the IL-6 family and corresponds to an additional signaling receptor binding site for LIFR in the case of CNTF, CLC, and NP.

The LIFR binding site is characterized by an F*XX*K motif located at the N terminus of the αD helix (36). The CNTF and CLC binding site 1 have been previously identified by site-directed mutagenesis (37, 38). These studies have shown that a conserved tryptophan residue and an R*XXX*D motif, which are located in the C-terminal parts of the AB loop and the αD helix, respectively, are required for CNTF and CLC interaction with CNTFRα. However, the counterpart of this contact site on CNTFRα is still unknown.

The aim of the present study was to determine the location of the binding site of CNTF, CLC, and NP on CNTFRα. For this purpose, NP was modeled, and its predicted binding site 1 was compared with the binding sites of CNTF and CLC. This analysis led us to identify a conserved binding site 1 among all of the CNTFRα ligands. Subsequently, the CNTFRα CBD was modeled, and its binding surface was analyzed to identify an area displaying physicochemical properties complementary to those of the CNTF, CLC, and NP binding site 1.

EXPERIMENTAL PROCEDURES

Sequence Alignments—CNTF, NP, CLC, LIF, cardiotrophin-1, oncostatin M, CNTFRα, IL-6Rα and IL-12p40 sequences were retrieved from the Uniprot and GenBank™ data bases. Multiple sequence alignments were obtained using the T-Coffee (available on the World Wide Web) and GeneDoc (available on the World Wide Web) programs. CNTFRα and NP secondary structures were predicted using Network Prediction Server @nalysis at the Pôle Bioinformatique Lyonnais (Lyon, France) (39). Multiple sequence alignments were also represented with WebLogo (available on the World Wide Web) (40).

Molecular Modeling—NP was modeled by satisfaction of spatial constraints using the Modeler program based on multiple sequence alignments and secondary structure predictions (41). The structural coordinates of human CNTF (42) and LIF (43) were selected as molecular templates for the four-helical core of NP; the coordinates of an additional α helix predicted in the AB loop of these cytokines were computed with the Biopolymer module of InsightII (Accelrys, San Diego, CA) and integrated during the modeling process.

CNTFRα was modeled as previously reported (21). Additional refinements of the CNTFRα model were carried out by optimizing side chain conformation using SCRWL3 (44). Electrostatic potentials were computed using Adaptive Poission-Boltzmann Solver with the AMBER force field (45, 46), and Eisenberg's hydrophobicity scale was used to display the protein surface hydrophobicity (47).

Protein Docking—CNTF, NP, and CNTFRα were manually superimposed onto their respective partner in the IL-6·IL-6Rα complex (Protein Data Bank accession number 1P9M) to build preliminary models. These models were further refined with the molecular docking program HEX 5.0 (48) to optimize structural complementarities. The best scoring solutions for each complex were energy-minimized with CHARMM (49) using the 100 steepest descent steps, followed by ABNR steps until a convergence gradient of 0.001 was reached.

Cells and Reagents—The COS-7, T98G glioblastoma, and SK-N-GP neuroblastoma cells were grown in RPMI 1640 medium supplemented with 10% fetal calf serum. The culture medium of Ba/F3 cells, modified to express the functional tripartite receptor for CNTF (BAF GLC), was supplemented with 5 ng/ml human CNTF (2). Anti-CNTFRα (AN-B2, AN-C2, and AN-E4) monoclonal antibodies and the polyclonal anti-CNTF

antibody were generated in the laboratory. The anti-protein C (HPC4) antibody was purchased from Roche Applied Science. The anti-STAT3 polyclonal antibody and the mAb-specific for phospho-705-STAT3 were from Santa Cruz Biotechnology, Inc. (Santa Cruz, CA) and New England Biolabs (Beverly, MA), respectively. CNTF, LIF, and IL-2 were bought from R&D Systems (Oxon, UK). CLC and mouse NP were produced as previously described (1, 2).

Site-directed Mutagenesis and Cell Transfection—The cDNAs encoding NP and the membrane or soluble forms of CNTFRα were subcloned in the pcDNA3.1 vector and subjected to site-directed mutagenesis using the QuikChange™ site-directed mutagenesis kit (Stratagene, La Jolla, CA), following the manufacturer's instructions. Mutations were verified by automatic DNA sequencing. cDNAs encoding mutant and wild type CNTFRα were transfected by electroporation in T98G glioblastoma cells using the Amaxa Nucleofactor™ technology (Amaxa, Köln, Germany), following the manufacturer's instructions. cDNAs encoding mutant and wild type (WT) NP were transfected in COS-7 cells, as previously described (1). After a 48-h culture period, cells or supernatants were harvested and assayed. Mutant and WT NP were purified from the supernatant, as previously described (1).

Tyrosine Phosphorylation Analysis and Western Blotting—Parental or transfected T98G cells and SK-N-GP neuroblastoma cells were activated for 10 min with the indicated cytokines before being lysed in 10 mM Tris-HCl, pH 7.6, 5 mM EDTA, 50 mM NaCl, 30 mM sodium pyrophosphate, 50 mM sodium fluoride, 1 mM sodium orthovanadate, protease inhibitors (1 μg/ml pepstatin, 2 μg/ml leupeptin, 5 μg/ml aprotinin, 1 mM phenylmethylsulfonyl fluoride), and 1% Nonidet P-40. The lysates were subjected to SDS-PAGE and immunoblot analysis with a mAb specific for the tyrosine-phosphorylated form of STAT3. Membranes were stripped in 0.1 M glycine, pH 2.5, for 15 h and neutralized in 1 M Tris-HCl, pH 7.6, before reblotting with an antibody recognizing all STAT3 isoforms.

Immunoprecipitation—COS-7 cell supernatants containing the wild type or mutated forms of soluble CNTFRα were harvested 48 h after transfection. For co-immunoprecipitation experiments, the receptors were incubated at a concentration of 1 nM with 1 nM CNTF. Then proteins were incubated overnight with the AN-C2 anti-CNTFRα mAb at a concentration of 10 μg/ml. Complexes were isolated using beads coupled to protein A, followed by SDS-PAGE. Western blot analyses were performed with an anti-protein C biotinylated mAb or an anti-CNTF biotinylated polyclonal antibody, and revealed by polystreptavidin peroxidase. The reaction was visualized using an image Master camera from Amersham Biosciences. Membranes were stripped as described above, before reblotting with the biotinylated anti-CNTFRα AN-E4 mAb.

Flow Cytometry Analysis—Parental and transfected T98G glioblastoma cells were incubated for 30 min at 4 °C with anti-CNTFRα monoclonal antibodies (AN-B2 and AN-C2) (10 μg/ml) or an isotype control antibody before using a phycoerythrin-conjugated anti-mouse antibody. CLC was biotin-tagged using the Bir A biotin ligase AviTag peptide substrate as previously described (50). CNTF and IL-2 were biotinylated using NHS-LC-biotin (Pierce). Binding of biotinylated CLC, CNTF, NP, or IL-2 as a control cytokine was revealed using phycoerythrin-labeled polystreptavidin for an additional 30-min incubation step. Fluorescence was subsequently analyzed on a FACScalibur flow cytometer (BD Biosciences).

Biological Assays—BAF GLC cells were seeded in 96-well plates at a concentration of 5×10^3 cells/well in RPMI 1640 medium containing 5% fetal calf serum. Serial dilutions of the cytokines tested were performed in triplicate. After a 72-h incubation period, 0.5 μCi of [^{3}H]Tdr was added to each well for the last 4 h of the culture, and the incorporated radioactivity was determined by scintillation counting, as previously described (51).

RESULTS

Analysis of the CNTF, CLC, and NP Binding Site 1 and NP Modeling—First, we performed a multiple sequence alignment of orthologs and paralogs of the IL-6 family members recruiting LIFR in their receptor complex (Fig. 2*A*). A conserved tryptophan residue (Trp^{64} and Trp^{94} in CNTF and CLC, respectively), located in the AB loop of these cytokines was previously reported to contribute to their binding site 1 (37, 38). The alignment shows that Trp^{85} in NP was highly conserved with CNTF Trp^{64} and CLC Trp^{94} and suggests that this residue is also involved in the NP site 1.

Additional residues in the αD helix of these cytokines also contribute to CNTF and CLC binding site 1 (37, 38). An R*XXX*D motif (Arg^{171} and Asp^{175} in CNTF and Arg^{197} and Asp^{201} in CLC) is conserved in the C-terminal part of this α helix. Interestingly, this R*XXX*D motif was also present in the C-terminal part of the NP αD helix (Arg^{190} and Asp^{194}). These observations suggested that, like CNTF and CLC, NP possesses a conserved binding site 1 for CNTFRα (Fig. 2*A*).

We built a NP molecular model using CNTF and LIF structures as templates. Next, we compared the NP model obtained with the CNTF structure or the CLC model previously reported (38, 42) and analyzed their binding site 1 (Fig. 2*B*). Strikingly, the NP binding surface involved a tryptophan residue located in the AB loop surrounded by positively charged residues, as already observed for CNTF and CLC. This clearly showed that the physicochemical properties of CNTF, CLC, and NP binding site 1 were conserved.

Site-directed Mutagenesis of NP—To confirm the modeling study, we generated the W85A NP mutant. As a control, an irrelevant F82A mutation, located in the vicinity of the area studied, was introduced into the NP sequence. WT and mutant forms of NP were expressed in the COS-7 cell line and purified on a Ni^{2+}-nitrilotriacetic acid column, as previously described (1). The functionality of WT NP and mutant NP was tested in a proliferation assay using the BAF GLC cell line expressing the tripartite CNTF receptor complex. The results showed a lack of proliferation when cells were grown in the presence of the W85A NP mutant compared with the proliferation observed in the presence of the WT or F82A forms of NP (Fig. 3*A*).

In addition, the NP mutants were studied for their ability to induce the recruitment of the STAT3 signaling pathway in SK-N-GP, a neuroblastoma cell line expressing the three CNTF receptor chains (Fig. 3*B*). A robust STAT3 tyrosine phosphorylation was observed in response to WT or F82A

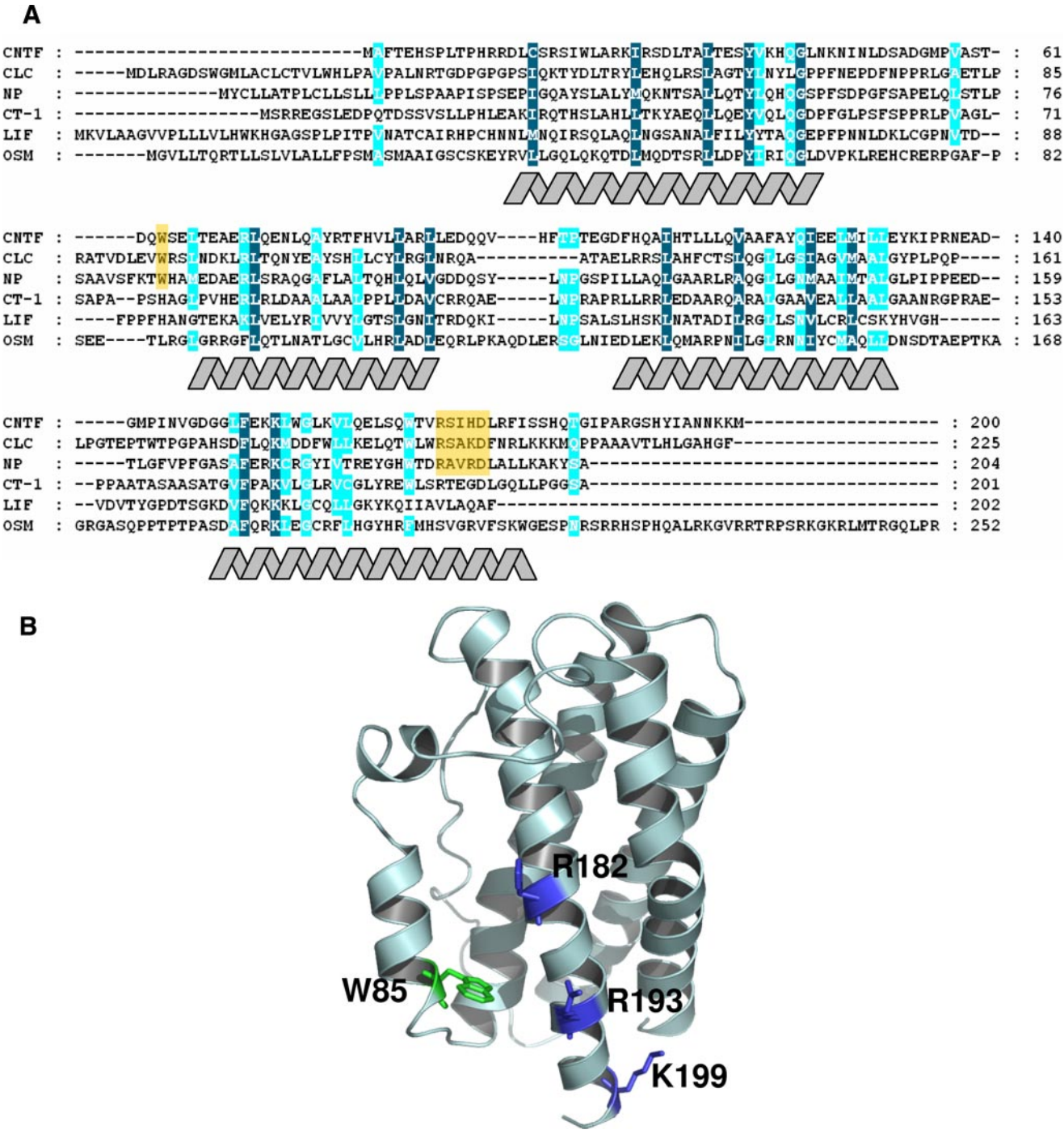

FIGURE 2. **Multiple sequence alignment of cytokines belonging to the IL-6 family and ribbon representation of the CNTF structure and CLC and NP models.** *A*, *dark blue-shaded letters* indicate conserved or type-conserved amino acids according to the BLOSUM45 matrix. 80% conserved residues are *shaded* in *cyan*. The NP sequence is murine, and the other sequences are human. The figure shows the assignment of the four α helices of the cytokines represented as predicted by the secondary structure prediction server Network. *Yellow boxes* highlight residues implicated in the CNTF, CLC, and NP binding site 1. *B*, *ribbon representation* of the NP model displaying charged and aromatic residues in its binding site. *Green residues*, aromatic amino acids; *blue residues*, polar and positively charged.

mutant forms of NP as well as to CNTF. In contrast, W85A NP mutant failed to activate STAT3. To conclude, Trp^{85} is a crucial residue for NP biological activities and is likely to contribute to the definition of a conserved site 1 among CNTF, CLC, and NP.

Molecular Modeling of CNTFRα—To identify counterpart(s) of the binding site 1 of CNTF, CLC, and NP on CNTFRα, we analyzed the CNTFRα model that we previously reported (21). For this purpose, we refined this model by optimizing the side chain conformation using SCRWL3.

Cytokine-receptor complexes, solved by x-ray crystallography (34, 52), have revealed that several receptor loops contain residues involved in their binding interfaces. Indeed, loops connecting β strands E and F, B′ and C′, and F′ and G′ are parts of

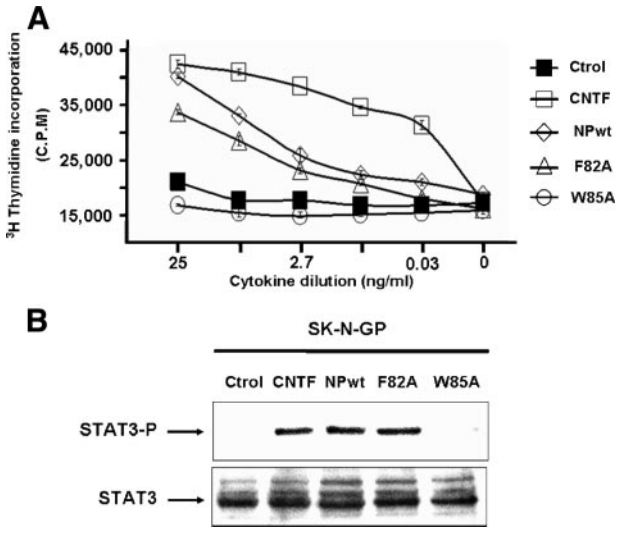

FIGURE 3. **Biological activities of purified wild type or mutant NP.** *A*, proliferation of the BAF GLC cell line in response to serial dilution of wild type (*white diamond*) or mutant NP as indicated: NP F82A (*white triangle*) or NP W85A (*white circle*). CNTF (*white square*) was used as a positive control. The *vertical bars* represent the S.E. *B*, analysis of STAT3 tyrosine phosphorylation levels in the SK-N-GP neuroblastoma cell line activated with 10 ng/ml wild type or mutant NP.

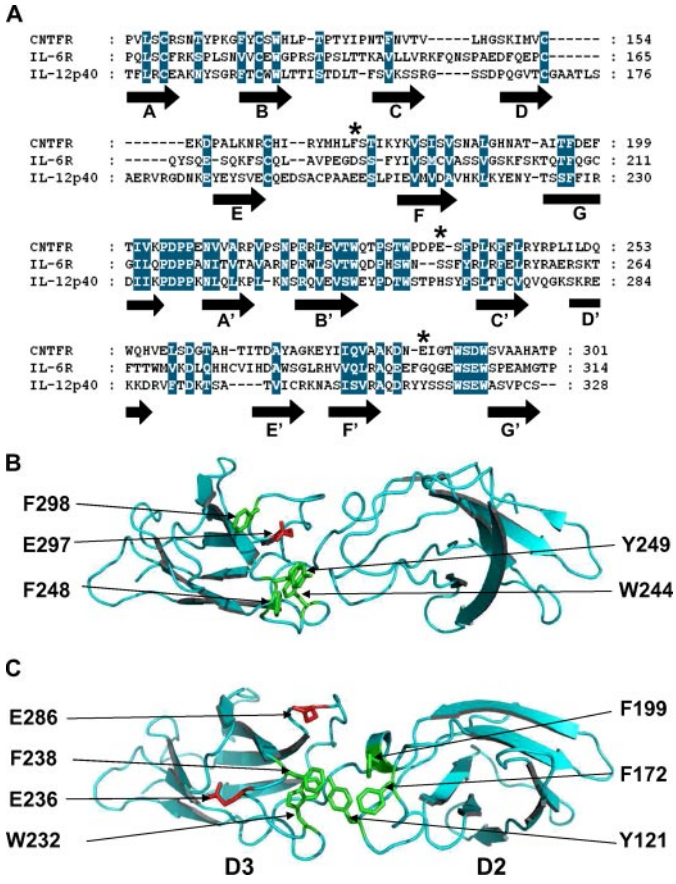

FIGURE 4. **Multiple sequence alignment of human CNTFRα, IL-6Rα and IL-12p40 CBD sequences and *ribbon representation* of the IL-6Rα CBD structure and the CNTFRα CBD model.** *A*, *dark blue-shaded letters* represent conserved or type-conserved amino acids according to the BLOSUM45 matrix. The figure shows the assignment of the β strands as predicted by the secondary structure prediction server Network. *Asterisks* highlight the positions of the predicted interacting residues of CNTFRα. *B*, *ribbon representation* of the IL-6Rα CBD. *C*, *ribbon representation* of the CNTFRα CBD. The side chains represented correspond to residues involved in the IL-6Rα binding site or predicted to be involved in the CNTFRα binding site. *Green residues*, aromatic amino acids; *red residues*, polar and negatively charged.

the receptor binding sites (34, 52, 53). This observation prompted us to carefully analyze these elements in CNTFRα.

We performed a multiple sequence alignment of CNTFRα with other short α chain receptor orthologs and paralogs, including IL-6Rα and IL-12p40 (Fig. 4*A*). This alignment showed that β strands were globally conserved between the different receptors as well as apolar residues involved in the hydrophobic core of the proteins. However, connecting loops, including EF, B′C′, and F′G′ loops, were not conserved between the different receptors.

Analysis of the CNTFRα model indicated that the hinge region connecting the D2 and D3 domains harbored an aromatic cluster composed of five residues (depicted in *green* in Fig. 4, *B* and *C*). These amino acids stabilized the CBD as commonly observed in this family of proteins (34, 52). However, we observed a structural divergence between the different α receptor chains when we analyzed the EF, B′C′, and F′G′ loops, which prevented identification of key CNTFRα interaction residues by homology with IL-6Rα and IL-12p40. Therefore, we studied the physicochemical properties of the CNTFRα surface and focused on the putative area(s) complementary to CNTF, CLC, and NP binding site 1.

Determination of the Putative CNTFRα Binding Site—To identify binding site complementary area(s), we computed and then compared the electrostatic potential of the CNTF and CNTFRα surfaces (Fig. 5). Indeed, residues Arg^{25} and Arg^{28}, located in the CNTF αA helix, mainly contributed to a positively charged area, as previously reported (37, 42). Fig. 5*C* shows the presence of an extended negatively charged surface centered on CNTFRα Glu^{236} and Glu^{286}, which forms a mirror image of the positively charged area of CNTF.

The hydrophobic potential was mapped onto the CNTF and CNTFRα surfaces. In agreement with previous studies (37, 42), Trp^{64} forms part of a hydrophobic pocket on the CNTF binding site 1 (Fig. 5*B*). A complementary residue, displaying similar physicochemical properties, was identified in the CBD hinge region of CNTFRα. It appears that the protruding side chain of Phe^{172} forms a hydrophobic patch complementary to the CNTF Trp^{64} pocket (Fig. 5*D*).

Moreover, we analyzed residue conservation in the EF, B′C′, and F′G′ interacting loops in different CNTFRα orthologs. Phe^{172}, Glu^{236}, and Glu^{286}, located in these loops, were evolutionary conserved or type conserved residues (Fig. 5*E*). These results further sustained the idea that the three residues identified were potential CNTFRα binding hot spots.

We also performed the same analyses for CLC and NP. Strikingly, CLC Trp^{94}, in agreement with our previous study (21), and NP Trp^{85} contributed to a hydrophobic pocket complementary to CNTFRα Phe^{172} (data not shown).

Molecular Docking of CNTFRα with Its Ligands—To further characterize the interaction of CNTFRα with its three ligands, molecular docking experiments were carried out. The IL-6·IL-6Rα complex was used as a template to build preliminary CNTF·CNTFRα and NP·CNTFRα models (the CLC·CNTFRα docking model was previously published (21)). The precise cytokine-receptor orientations were computed using HEX to

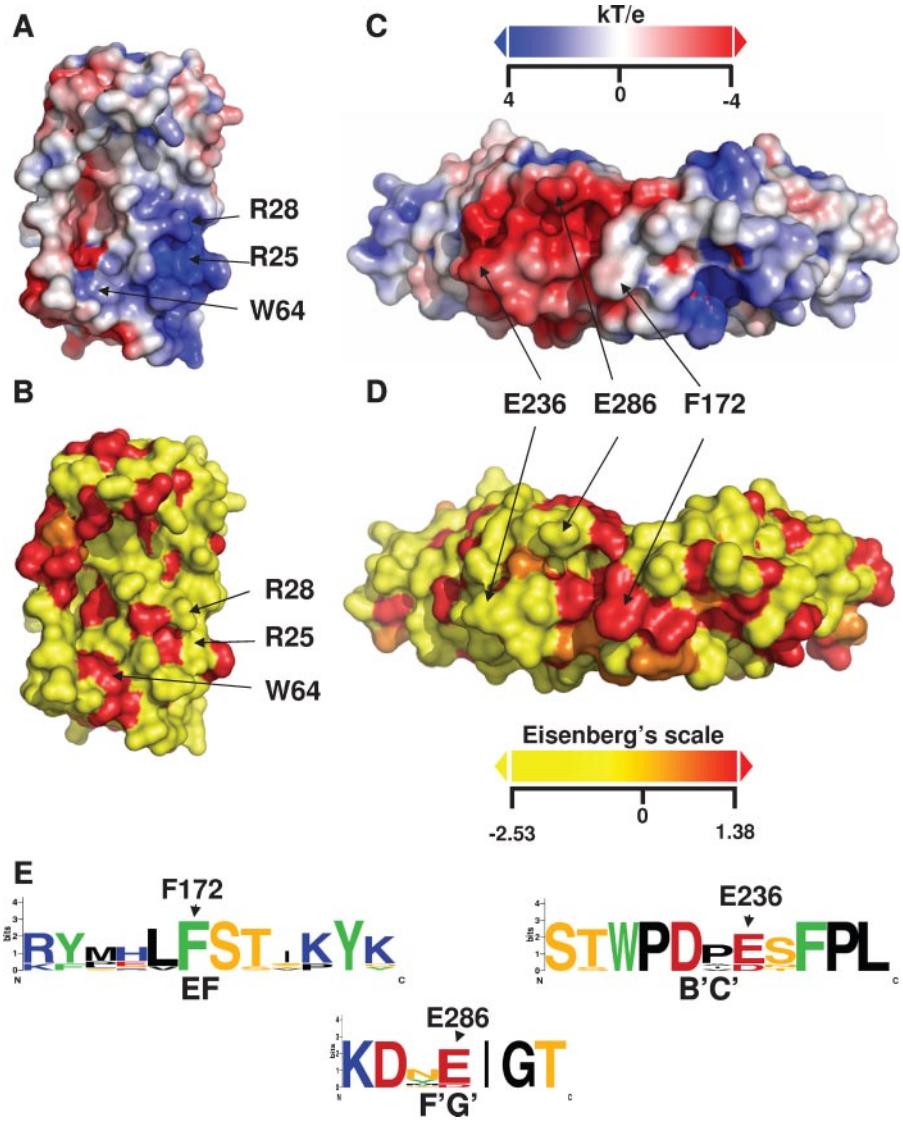

FIGURE 5. **Connolly surfaces of CNTF (*A* and *B*) and of the CNTFRα CBD (*C* and *D*) and residue conservation of CNTFRα-interacting loops (*E*).** The electrostatic potentials (*A* and *C*) and the hydrophobic index of the exposed residues (*B* and *D*) were mapped onto the surfaces of CNTF and CNTFRα as described under "Experimental Procedures." The orientations of CNTF and CNTFRα have been manually adjusted to provide an "open book" surface representation of the interfaces. *E*, conservation of residues present in CNTFRα-interacting loops are represented as *logos*. Each *logo* consists of *stacks* of *symbols*, one *stack* for each position in the sequence. The overall *height* of the *stack* indicates the sequence conservation at that position, whereas the *height* of *symbols* within the *stack* indicates the relative frequency of each amino acid at that position. *Green residues*, aromatic amino acids; *blue residues*, polar and positively charged; *red residues*, polar and negatively charged; *black residues*, hydrophobic; *orange residues*, polar and neutral.

optimize protein shape complementarities. Complexes with the best scoring solutions were then energy minimized to allow side chain reorientation at the cytokine-receptor interface. The CNTF·CNTFRα complex model is presented in Fig. 6 (the NP·CNTFRα complex appears as supplemental Fig. 1).

This model shows that the CNTF Trp^{64} and CNTFRα Phe^{172} are involved in an aromatic-aromatic interaction. In the vicinity of this hydrophobic area, a cluster of polar residues is formed by CNTF Arg^{25} and Arg^{28} located in the αA helix and CNTFRα Glu^{236} and Glu^{286} located in the D3 domain. These residues are predicted to form salt bridges between the two proteins. Additional charged residues (CNTF Arg^{177} and CNTFRα Asp^{234}) might also contribute to the interaction by long range electrostatic effects. Similarly, CNTFRα Glu^{236} and Glu^{286} were also predicted to be involved in salt bridge or hydrogen bond with polar NP residues.

Site-directed Mutagenesis and Expression of the Mutated Forms of CNTFRα—Based on the above observations, we selected Phe^{172}, Glu^{236}, and Glu^{286} of CNTFRα as important residues for interaction with its different cognate ligands. Mutants were designed to alter the receptor binding capacities, and the following mutations were introduced: F172A, E236A, and E286A. In addition, Phe^{199} located in the vicinity of the potentially critical residue Phe^{172} was also mutated to alanine and used as irrelevant control for our model.

Corresponding cDNAs were transfected in the T98G human glioblastoma, a cell line expressing gp130 and LIFR, but not CNTFRα (1). A strong expression of both WT and mutated forms of CNTFRα was detected by FACS analysis (Fig. 7). A similar expression level was observed using either AN-B2 or AN-C2 antibody, two mAbs directed against different CNTFRα conformational epitopes (20). This finding indicates that the mutations introduced did not significantly alter CNTFRα folding and structure (Fig. 7).

Binding Properties of CNTFRα Mutants—The binding properties of CNTFRα mutants expressed in the T98G glioblastoma cell line were examined. For this purpose, CNTF and CLC were biotinylated and incubated with the transfected cells. Binding to the cell surface was monitored by fluorescence-activated cell sorting analysis (Fig. 8). Readily detectable signals were measured when either CLC or CNTF was incubated with cells expressing WT CNTFRα or the F199A mutant. As expected, no binding could be detected when either CNTF or CLC were incubated with the T98G parental cell line. Importantly, a significant decrease or complete abrogation of CNTF and CLC binding was observed when the cytokines were added to the cells expressing either E286A or F172A forms of CNTFRα. In contrast, no significant change in cytokine interaction was seen for the E236A mutant (Fig. 8). Similar biotinylation experiments were carried out with NP, but major protein instability was observed during the labeling process. Therefore, we could not perform the binding analyses (data not shown). Together, these results indicate that CNTFRα Phe^{172} and Glu^{286} play an important role in CLC and

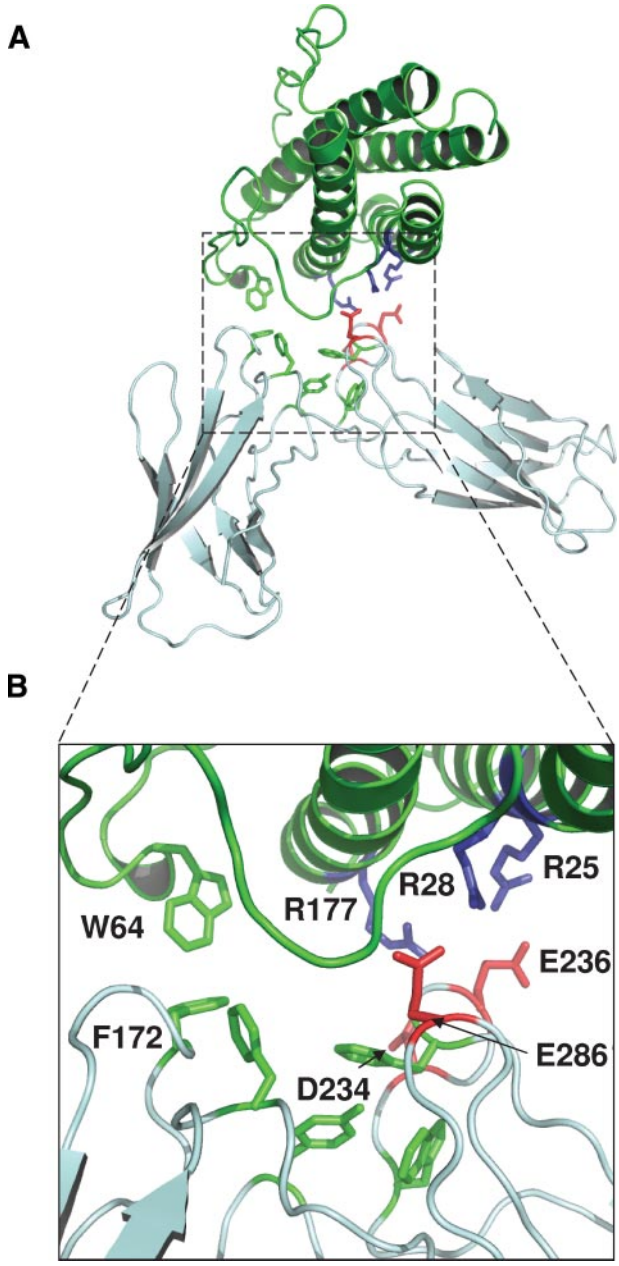

FIGURE 6. **Molecular docking of CNTF with CNTFRα.** *A*, *ribbon representation* of the CNTF (*green*)·CNTFRα (*cyan*) complex model. *B*, close-up view of the predicted interface showing the interacting residues. *Green residues*, aromatic amino acids; *blue residues*, polar and positively charged; *red residues*, polar and negatively charged.

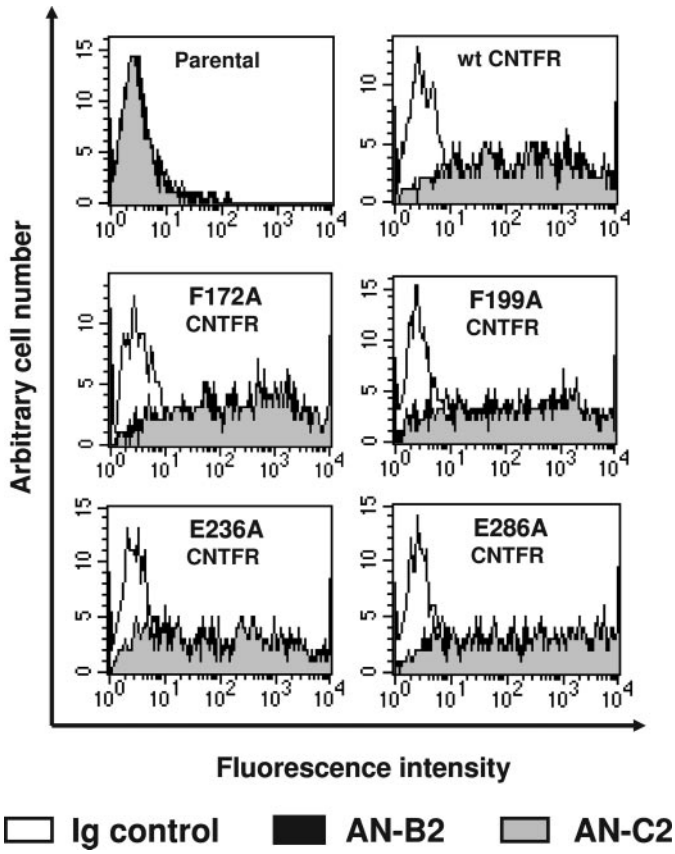

FIGURE 7. **Wild type and mutant membrane CNTFRα receptor expression in transfected T98G glioblastoma cells and analyzed by flow cytometry.** *Dark* and *gray histograms* represent CNTFRα expression analyzed with AN-B2 or AN-C2 anti-CNTFRα mAbs, respectively (*gray histograms* largely overlaid the *black histograms*). *White histograms* correspond to the isotype control antibody.

CNTF binding, in agreement with our molecular modeling study.

Mutant CNTFRα Association with CNTF and CLC—Previous studies have shown that a soluble form of CNTFRα can bind CNTF (20, 26). To monitor the interaction of soluble CNTFRα with CNTF, co-immunoprecipitation experiments were performed (Fig. 9*A*). Results showed that the soluble CNTFRα F172A and E286A mutants failed to interact with CNTF compared with the WT or F199A forms used as a control.

We previously reported that CLC was secreted as a composite cytokine when associated with a soluble receptor moiety that could be either cytokine-like factor 1 or soluble CNTFRα (2, 20). We studied the interaction between CLC and soluble CNTFRα by co-expressing a tagged form of the cytokine together with the soluble receptor mutants in the COS-7 cell line. Co-immunoprecipitation experiments showed the secretion of a stable composite when CLC was co-expressed either with WT or F199A mutant (Fig. 9*B*). Interestingly, no stable heterocomplex formation of CLC with the F172A or E286A soluble receptors could be detected. However, a slight secretion of CLC was observed when co-expressed with the E286A CNTFRα mutant. This result underlines a transient interaction between the two proteins in agreement with the results presented in Fig. 8. Analysis of cell lysates confirmed the correct expression of both partner proteins. NP interaction with soluble CNTFRα mutants could not be assessed, since we previously reported that NP only recognized the membrane form of CNTFRα (1). These results indicate that CNTF and CLC interact predominantly with CNTFRα through the same residues, Phe^{172} and Glu^{286}.

Functional Properties of CNTFRα Mutants—We examined the functional properties of CNTFRα mutants in response to CNTF, CLC, and NP. We analyzed the tyrosine phosphorylation level of STAT3, a major signaling pathway recruited by the tripartite CNTF receptor complex. Experiments were carried out using the T98G glioblastoma cell line transfected with CNTFRα mutants. LIF, which mediates its responses through

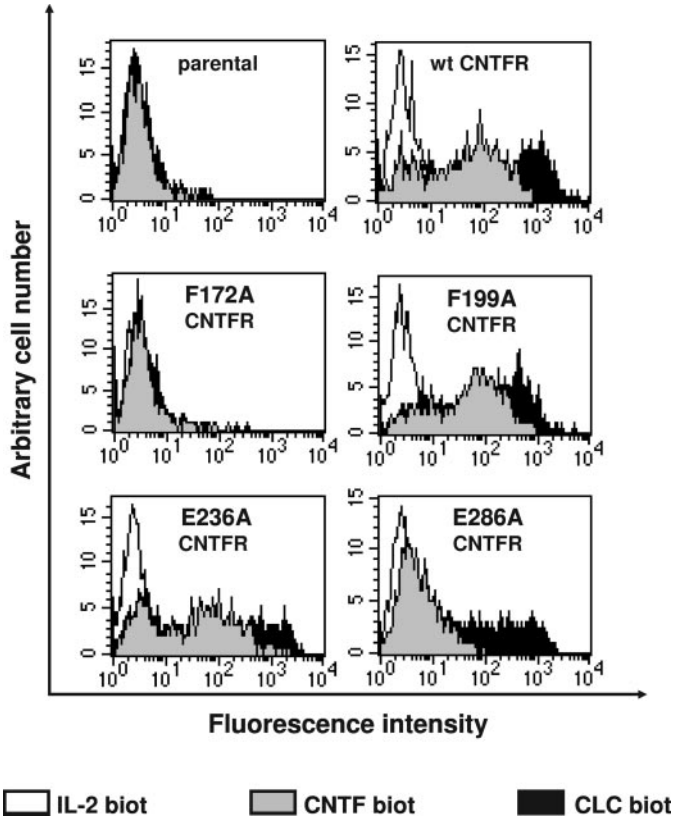

FIGURE 8. **Binding of CNTF and CLC on T98G glioblastoma cells transfected with wild type or mutant CNTFRα receptors and analyzed by flow cytometry.** *White histograms* correspond to the control signals. *Gray* and *dark histograms* represent CNTF and CLC binding, respectively.

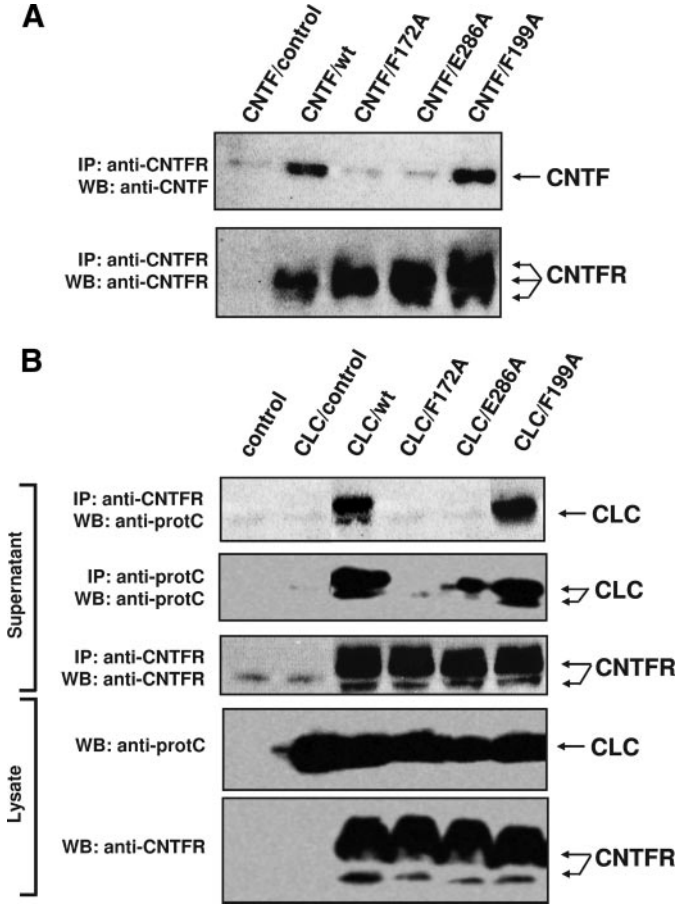

FIGURE 9. **Co-immunoprecipitation of CNTF and CLC and secretion of CLC with mutant forms of CNTFRα.** *A*, 1 nM soluble wild type or mutant CNTFRα and CNTF were immunoprecipitated (*IP*) using the anti-CNTFRα (AN-C2) mAb, and CNTF was visualized by Western blot (*WB*). *B*, mutant or WT soluble CNTFRα was co-synthesized with a protein C-tagged form of CLC in COS-7 cells to allow for the formation of the composite cytokine. Culture supernatants were harvested before immunoprecipitation of the CLC·CNTFRα complex using the anti-CNTFRα (AN-C2) mAb or CLC using the anti-protein C mAb. CLC was then visualized by Western blot using the anti-protein C antibody. The presence of CLC and CNTFRα was also controlled in the lysate of the transfected cells. Membranes were stripped before reblotting with the biotinylated anti-CNTFR AN-E4 mAb as a control.

the gp130·LIFR heterocomplex, was used as a positive control (Fig. 10).

Western blot assays showed that CNTFRα is necessary to induce STAT3 phosphorylation in response to CNTF, CLC, or NP. A nearly total extinction of the signal was observed when cells were transfected with F172A or E286A receptor mutants and activated with CNTFRα ligands. In the cells expressing the E236A mutant or the F199A mutant, the STAT3 pathway remained sensitive to stimulation with the three ligands. These combined results corroborate the modeling and binding results of the study.

DISCUSSION

CNTFRα is able to specifically recognize three different ligands sharing 16–25% sequence identity. Previous studies have identified binding site 1 of CNTF and CLC (37, 38), but its counterpart on CNTFRα has not yet been described to date regarding the binding site 1 counterpart on CNTFRα. We therefore undertook the identification of the molecular determinants implicated in the interaction of CNTFRα with its ligands, in order to understand its cross-reactivity.

The resolution of cytokine-receptor complexes by crystallography has determined the molecular assembly of this family of proteins (34, 52–54). It first revealed that this protein-protein assembly requires complementary shapes and physicochemical properties. Moreover, site-directed mutagenesis experiments have demonstrated that only a few residues, defined as interac-

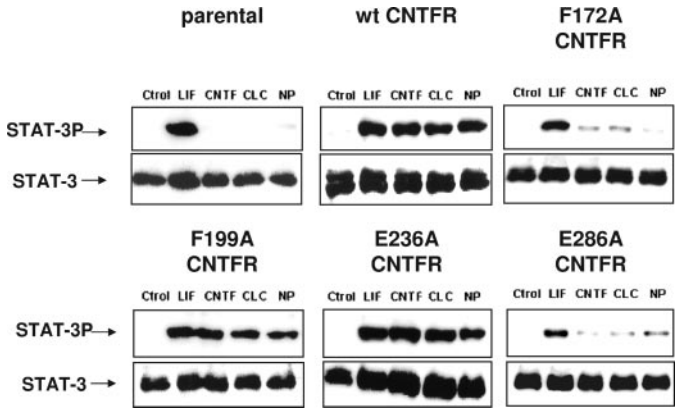

FIGURE 10. **Induction of STAT3 tyrosine phosphorylation in T98G cells transfected with wild type or mutant CNTFRα.** Parental and transfected T89G glioblastoma cells were incubated for 10 min with 1 ng/ml LIF, CNTF, CLC, or NP, as indicated. Cells were then lysed and subjected to Western blotting using an anti-phospho-STAT3 (*STAT-3P*) or an anti-STAT-3 (*STAT-3*) antibody.

tion hot spots, contribute to the binding free energy (55). Statistical analyses of numerous receptor binding sites have revealed that hot spots are often conserved and are significantly enriched in aromatic amino acids (56).

These notions were used to look for the complementary site 1 of CNTFRα. In the present study, we have shown that CNTF, CLC, and NP share the same binding site 1. The CNTFRα putative structural binding epitope was determined by searching a surface area with physicochemical properties complementary to the binding site 1 of CNTF, CLC, and NP. To reinforce the modeling prediction, the residues identified were substituted with alanine, and the mutants obtained were further tested in a panel of biological assays.

Both Panayotatos's group and ours previously reported the involvement of the conserved residues CNTF Trp^{64} and CLC Trp^{94} for the interaction of these cytokines with CNTFRα (37, 38). Additional residues also contribute to CNTF and CLC binding site 1. An R*XXX*D motif (CNTF Arg^{171} and Asp^{175} and CLC Arg^{197} and Asp^{201}) is conserved in their αD helix and is essential for the side chain orientation of the tryptophan residue hot spot (37, 42). Furthermore, we have identified inactivating mutations in the gene coding for CLC in a patient suffering from cold-induced sweating syndrome (21). One of these mutations, a substitution of Arg^{197}, impairs the CLC/CNTFRα interaction. This observation confirms the importance of R*XXX*D motif for the integrity of binding site 1.

In the present study, we characterized the NP binding site 1, which is conserved across the three CNTFRα ligands. The NP Trp^{85} residue, equivalent to CNTF Trp^{64} and CLC Trp^{94}, was found to be a hot spot at the interface of the NP·CNTFRα complex. Interestingly, an R*XXX*D motif was also conserved in the αD helix of NP (Arg^{190} and Asp^{194}). The determination of a conserved site 1 for CNTF, CLC, and NP was the starting point for our investigation of the CNTFRα binding epitope.

The structural diversity of the receptor-interacting loops led us to compute surface physicochemical properties of CNTFRα in order to identify complementarities with CNTF, CLC, and NP binding surfaces. A mirror image of the three cytokines' binding site 1 was found on CNTFRα. The residues, Phe^{172}, Glu^{236}, and Glu^{286}, were identified as potential components of its binding epitope. Our study clearly established that the F172A and E286A CNTFRα mutations impaired or decreased CNTF, CLC, and NP interactions.

The F172A mutation in the EF loop of the CNTFRα domain completely abrogated the binding of CNTF, CLC, and NP with this receptor. Moreover, the CNTFRα F172A mutant failed to mediate biological responses induced by these three cytokines. These results confirmed the data obtained with CNTF W64A, CLC W94A, and NP W85A mutants (37, 38). Our docking study indicated that these tryptophan residues were involved in aromatic-aromatic interactions with CNTFR Phe^{172}. The highly disruptive effects of corresponding mutations further confirmed that Phe^{172} was a hot spot residue on the CNTFRα surface.

Similarly, the E286A mutation impaired biological activity mediated through CNTFRα in response to CNTF, CLC, and NP. A salt bridge between CNTF Arg^{25} and CNTFRα Glu^{286} was observed in the CNTF·CNTFRα complex model that we generated. These observations fit with results obtained with the CNTF Arg^{25} mutant, which also lost its CNTFRα recognition capacity (37).

Analysis of the related cytokine-receptor α chain complexes shows that aromatic-aromatic and salt bridge interactions are globally conserved at these protein interfaces (34, 52). In the IL-6·IL-6Rα structure, the IL-6Rα Phe^{248} residue is critical for the interaction with IL-6 Phe^{106} located in the cytokine AB loop, as supported by mutational experiments (34, 57). A similar situation was observed for IL-12p35·IL-12p40, where the IL-12p40 Tyr^{246} residue and its paring residue (Tyr^{193}) present in the αD helix of p35 were found to be important in the interaction of the IL-12p35 and IL-12p40 subunits (52). Conserved salt bridges between IL-6 Arg^{207} and IL-6Rα Glu^{296} or IL-12p35 Arg^{239} and IL-12p40 Glu^{203} are also important for cytokine-receptor binding.

The present work, as well as previous studies (34, 52), suggests that despite structural divergence of receptor-interacting loops, the different cytokines and receptors of the IL-6/IL-12 family have kept similar intermolecular interactions in order to associate with each other. Importantly, conserved pairs of aromatic or charged residues on these protein interfaces seem to be a conserved feature of cytokines and receptors interacting through a binding site 1 in the IL-6/IL-12 family. This finding could help to identify crucial residues involved in the interactions of newly described composite cytokine subunits, such as IL-23, IL-27, or IL-35 (6, 58–60).

In conclusion, CNTF, CLC, and NP share an overlapping binding epitope located in the CNTFRα CBD and involving Phe^{172} and Glu^{286} residue hot spots. The CNTFRα Phe^{172} residue is the mirror image of the conserved tryptophan hot spot identified in CNTF, CLC, and NP. These pairs of residues are predicted to form an aromatic-aromatic interaction at the cytokine/receptor interface. The CNTFRα Glu^{286} residue is a hot spot residue at the CNTF/CNTFRα and NP/CNTFRα interfaces and plays a major role in CLC·CNTFRα complex stability.

Acknowledgments—We thank G. Elson for careful review of the manuscript and D. Perret for stimulating discussions in the early phase of the project.

REFERENCES

1. Derouet, D., Rousseau, F., Alfonsi, F., Froger, J., Hermann, J., Barbier, F., Perret, D., Diveu, C., Guillet, C., Preisser, L., Dumont, A., Barbado, M., Morel, A., deLapeyriere, O., Gascan, H., and Chevalier, S. (2004) *Proc. Natl. Acad. Sci. U. S. A.* **101,** 4827–4832
2. Elson, G. C., Lelievre, E., Guillet, C., Chevalier, S., Plun-Favreau, H., Froger, J., Suard, I., de Coignac, A. B., Delneste, Y., Bonnefoy, J. Y., Gauchat, J. F., and Gascan, H. (2000) *Nat. Neurosci.* **3,** 867–872
3. Heinrich, P. C., Behrmann, I., Muller-Newen, G., Schaper, F., and Graeve, L. (1998) *Biochem. J.* **334,** 297–314
4. Peters, M., Muller, A. M., and Rose-John, S. (1998) *Blood* **92,** 3495–3504
5. Taga, T., and Kishimoto, T. (1997) *Annu. Rev. Immunol.* **15,** 797–819
6. Pflanz, S., Timans, J. C., Cheung, J., Rosales, R., Kanzler, H., Gilbert, J., Hibbert, L., Churakova, T., Travis, M., Vaisberg, E., Blumenschein, W. M., Mattson, J. D., Wagner, J. L., To, W., Zurawski, S., McClanahan, T. K., Gorman, D. M., Bazan, J. F., de Waal Malefyt, R., Rennick, D., and Kastelein, R. A. (2002) *Immunity* **16,** 779–790
7. Bazan, J. F. (1991) *Neuron* **7,** 197–208
8. Curtis, R., Adryan, K. M., Zhu, Y., Harkness, P. J., Lindsay, R. M., and DiStefano, P. S. (1993) *Nature* **365,** 253–255

9. Lin, L. F., Mismer, D., Lile, J. D., Armes, L. G., Butler, E. T., III, Vannice, J. L., and Collins, F. (1989) *Science* **246,** 1023–1025
10. Mitsumoto, H., Ikeda, K., Klinkosz, B., Cedarbaum, J. M., Wong, V., and Lindsay, R. M. (1994) *Science* **265,** 1107–1110
11. Oppenheim, R. W., Prevette, D., Yin, Q. W., Collins, F., and MacDonald, J. (1991) *Science* **251,** 1616–1618
12. Sendtner, M., Schmalbruch, H., Stockli, K. A., Carroll, P., Kreutzberg, G. W., and Thoenen, H. (1992) *Nature* **358,** 502–504
13. Stockli, K. A., Lottspeich, F., Sendtner, M., Masiakowski, P., Carroll, P., Gotz, R., Lindholm, D., and Thoenen, H. (1989) *Nature* **342,** 920–923
14. Linker, R. A., Maurer, M., Gaupp, S., Martini, R., Holtmann, B., Giess, R., Rieckmann, P., Lassmann, H., Toyka, K. V., Sendtner, M., and Gold, R. (2002) *Nat. Med.* **8,** 620–624
15. Guillet, C., Auguste, P., Mayo, W., Kreher, P., and Gascan, H. (1999) *J. Neurosci.* **19,** 1257–1262
16. Helgren, M. E., Squinto, S. P., Davis, H. L., Parry, D. J., Boulton, T. G., Heck, C. S., Zhu, Y., Yancopoulos, G. D., Lindsay, R. M., and DiStefano, P. S. (1994) *Cell* **76,** 493–504
17. Duff, E., and Baile, C. A. (2003) *Nutr. Rev.* **61,** 423–426
18. Kokoeva, M. V., Yin, H., and Flier, J. S. (2005) *Science* **310,** 679–683
19. Senaldi, G., Varnum, B. C., Sarmiento, U., Starnes, C., Lile, J., Scully, S., Guo, J., Elliott, G., McNinch, J., Shaklee, C. L., Freeman, D., Manu, F., Simonet, W. S., Boone, T., and Chang, M. S. (1999) *Proc. Natl. Acad. Sci. U. S. A.* **96,** 11458–11463
20. Plun-Favreau, H., Elson, G., Chabbert, M., Froger, J., deLapeyriere, O., Lelievre, E., Guillet, C., Hermann, J., Gauchat, J. F., Gascan, H., and Chevalier, S. (2001) *EMBO J.* **20,** 1692–1703
21. Rousseau, F., Gauchat, J. F., McLeod, J. G., Chevalier, S., Guillet, C., Guilhot, F., Cognet, I., Froger, J., Hahn, A. F., Knappskog, P. M., Gascan, H., and Boman, H. (2006) *Proc. Natl. Acad. Sci. U. S. A.* **103,** 10068–10073
22. Davis, S., Aldrich, T. H., Stahl, N., Pan, L., Taga, T., Kishimoto, T., Ip, N. Y., and Yancopoulos, G. D. (1993) *Science* **260,** 1805–1808
23. Davis, S., Aldrich, T. H., Valenzuela, D. M., Wong, V. V., Furth, M. E., Squinto, S. P., and Yancopoulos, G. D. (1991) *Science* **253,** 59–63
24. Gearing, D. P., Thut, C. J., VandeBos, T., Gimpel, S. D., Delaney, P. B., King, J., Price, V., Cosman, D., and Beckmann, M. P. (1991) *EMBO J.* **10,** 2839–2848
25. Hibi, M., Murakami, M., Saito, M., Hirano, T., Taga, T., and Kishimoto, T. (1990) *Cell* **63,** 1149–1157
26. Davis, S., Aldrich, T. H., Ip, N. Y., Stahl, N., Scherer, S., Farruggella, T., DiStefano, P. S., Curtis, R., Panayotatos, N., Gascan, H., Chevalier, S., and Yancopoulos, G. D. (1993) *Science* **259,** 1736–1739
27. Robledo, O., Auguste, P., Coupey, L., Praloran, V., Chevalier, S., Pouplard, A., and Gascan, H. (1996) *J. Neurochem.* **66,** 1391–1399
28. Lutticken, C., Wegenka, U. M., Yuan, J., Buschmann, J., Schindler, C., Ziemiecki, A., Harpur, A. G., Wilks, A. F., Yasukawa, K., Taga, T., Kishimoto, T., Barbieri, G., Pelligrini, S., Sendtner, M., Heinrich, P., and Horn, F. (1994) *Science* **263,** 89–92
29. Stahl, N., Boulton, T. G., Farruggella, T., Ip, N. Y., Davis, S., Witthuhn, B. A., Quelle, F. W., Silvennoinen, O., Barbieri, G., and Pellegrini, S. (1994) *Science* **263,** 92–95
30. Stahl, N., Farruggella, T. J., Boulton, T. G., Zhong, Z., Darnell, J. E., Jr., and Yancopoulos, G. D. (1995) *Science* **267,** 1349–1353
31. Bazan, J. F. (1990) *Proc. Natl. Acad. Sci. U. S. A.* **87,** 6934–6938
32. Bravo, J., and Heath, J. K. (2000) *EMBO J.* **19,** 2399–2411
33. Boulanger, M. J., and Garcia, K. C. (2004) *Adv. Protein Chem.* **68,** 107–146
34. Boulanger, M. J., Chow, D. C., Brevnova, E. E., and Garcia, K. C. (2003) *Science* **300,** 2101–2104
35. de Vos, A. M., Ultsch, M., and Kossiakoff, A. A. (1992) *Science* **255,** 306–312
36. Plun-Favreau, H., Perret, D., Diveu, C., Froger, J., Chevalier, S., Lelievre, E., Gascan, H., and Chabbert, M. (2003) *J. Biol. Chem.* **278,** 27169–27179
37. Panayotatos, N., Radziejewska, E., Acheson, A., Somogyi, R., Thadani, A., Hendrickson, W. A., and McDonald, N. Q. (1995) *J. Biol. Chem.* **270,** 14007–14014
38. Perret, D., Guillet, C., Elson, G., Froger, J., Plun-Favreau, H., Rousseau, F., Chabbert, M., Gauchat, J. F., and Gascan, H. (2004) *J. Biol. Chem.* **279,** 43961–43970
39. Deleage, G., Blanchet, C., and Geourjon, C. (1997) *Biochimie* (*Paris*) **79,** 681–686
40. Crooks, G. E., Hon, G., Chandonia, J. M., and Brenner, S. E. (2004) *Genome Res.* **14,** 1188–1190
41. Sali, A., and Blundell, T. L. (1993) *J. Mol. Biol.* **234,** 779–815
42. McDonald, N. Q., Panayotatos, N., and Hendrickson, W. A. (1995) *EMBO J.* **14,** 2689–2699
43. Robinson, R. C., Grey, L. M., Staunton, D., Vankelecom, H., Vernallis, A. B., Moreau, J. F., Stuart, D. I., Heath, J. K., and Jones, E. Y. (1994) *Cell* **77,** 1101–1116
44. Canutescu, A. A., Shelenkov, A. A., and Dunbrack, R. L., Jr. (2003) *Protein Sci.* **12,** 2001–2014
45. Baker, N. A., Sept, D., Joseph, S., Holst, M. J., and McCammon, J. A. (2001) *Proc. Natl. Acad. Sci. U. S. A.* **98,** 10037–10041
46. Case, D. A., Cheatham, T. E., III, Darden, T., Gohlke, H., Luo, R., Merz, K. M., Jr., Onufriev, A., Simmerling, C., Wang, B., and Woods, R. J. (2005) *J. Comput. Chem.* **26,** 1668–1688
47. Eisenberg, D., Weiss, R. M., and Terwilliger, T. C. (1984) *Proc. Natl. Acad. Sci. U. S. A.* **81,** 140–144
48. Mustard, D., and Ritchie, D. W. (2005) *Proteins* **60,** 269–274
49. Brooks, B. R., Bruccoleri, R. E., Olafson, B. D., States, D. J., Swaminathan, S., and Karplus, M. (1983) *J. Comp. Chem.* **4,** 187–217
50. Cognet, I., Guilhot, F., Gabriac, M., Chevalier, S., Chouikh, Y., Herman-Bert, A., Guay-Giroux, A., Corneau, S., Magistrelli, G., Elson, G. C., Gascan, H., and Gauchat, J. F. (2005) *J. Immunol. Methods* **301,** 53–65
51. Chevalier, S., Fourcin, M., Robledo, O., Wijdenes, J., Pouplard-Barthelaix, A., and Gascan, H. (1996) *J. Biol. Chem.* **271,** 14764–14772
52. Yoon, C., Johnston, S. C., Tang, J., Stahl, M., Tobin, J. F., and Somers, W. S. (2000) *EMBO J.* **19,** 3530–3541
53. Boulanger, M. J., Bankovich, A. J., Kortemme, T., Baker, D., and Garcia, K. C. (2003) *Mol. Cell* **12,** 577–589
54. Chow, D., He, X., Snow, A. L., Rose-John, S., and Garcia, K. C. (2001) *Science* **291,** 2150–2155
55. Bravo, J., Staunton, D., Heath, J. K., and Jones, E. Y. (1998) *EMBO J.* **17,** 1665–1674
56. Ma, B., Elkayam, T., Wolfson, H., and Nussinov, R. (2003) *Proc. Natl. Acad. Sci. U. S. A.* **100,** 5772–5777
57. Kalai, M., Montero-Julian, F. A., Grotzinger, J., Fontaine, V., Vandenbussche, P., Deschuyteneer, R., Wollmer, A., Brailly, H., and Content, J. (1997) *Blood* **89,** 1319–1333
58. Collison, L. W., Workman, C. J., Kuo, T. T., Boyd, K., Wang, Y., Vignali, K. M., Cross, R., Sehy, D., Blumberg, R. S., and Vignali, D. A. (2007) *Nature* **450,** 566–569
59. Devergne, O., Birkenbach, M., and Kieff, E. (1997) *Proc. Natl. Acad. Sci. U. S. A.* **94,** 12041–12046
60. Oppmann, B., Lesley, R., Blom, B., Timans, J. C., Xu, Y., Hunte, B., Vega, F., Yu, N., Wang, J., Singh, K., Zonin, F., Vaisberg, E., Churakova, T., Liu, M., Gorman, D., Wagner, J., Zurawski, S., Liu, Y., Abrams, J. S., Moore, K. W., Rennick, D., de Waal-Malefyt, R., Hannum, C., Bazan, J. F., and Kastelein, R. A. (2000) *Immunity* **13,** 715–725